Interaction Notes

Note 103

May 26, 1972

Induced Electric Currents on Configurations of Thick Wires

Perpendicular Crossed Wires

Thomas H. Shumpert
Terry T. Crow
Mississippi State University
State College, Mississippi 39762

Clayborne D. Taylor
University of Mississippi
University, Mississippi 38677

thick wires, conductors, induced current, effects of EMP

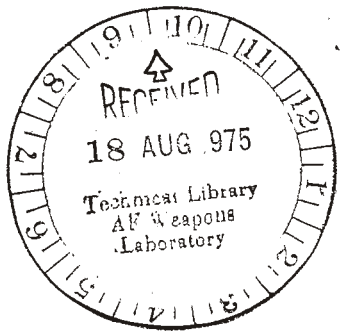

Induced Electric Currents on Configurations

of Thick Wires

Perpendicular Crossed Wires

ABSTRACT

The general theory previously developed is extended to a consideration of thick wire structures by adding so-called end current corrections to the set of general integral equations for the system of wires. Perfectly conducting flat end caps having a uniform charge distribution are placed on the free ends of each wire. These charges contribute additional terms in the scalar potential expressions and significantly affect the current distributions on wires having small length to radius ratios.

FORWARD

Numerical results are presented and compared to thin wire theory in a series of graphs at the end of the report. We express our appreciation to Dr. Carl Baum for his continuing interest in this type problem and for his comments and suggestions during the course of the work.

1. Introduction

In a series of papers and Interactions Notes, coupled integral equations predicting the electrical behavior of a series of wires have been developed and reviewed [1,2,3,4,5,6]. In the present development additional terms involving other end current corrections are added to the equations to account for the finite thickness of the wires. These terms play a significant role in determining the form of the current distributions near the ends of so-called thick wire structures.

2. Discussion

In a continuing effort to model more accurately an aircraft, a development is outlined which attempts to account for the finite thickness of wires used to approximate the structure. In an earlier Note [3] the derivation of the integral equations is reviewed and the results of a parameter study are presented. This work clearly indicated the need for additional considerations to handle so-called thick structures. The approach used to simulate the thick wire structure is to assume the existence of perfectly conducting flat end caps on the free ends of each wire cylinder present in the system. A recent note [6] considered the possibility of non-zero end currents on structures but for a different application.

In terms of charge distributions the scalar potential on the n-th wire of a system containing N wires can be written as

$$\phi_n(S_n) = \frac{1}{4\pi\varepsilon} \sum_{m=1}^{N} \left\{ \int_{L_m^1}^{L_m^u} \rho(S_m')G(S_n, S_m')dS_m' \right.$$

$$+ \int_0^{a_m} \sigma(r_m', L_m^u)G(r_m', L_m^u, S_n)2\pi r_m' dr_m'$$

$$\left. \int^{a_m} \right)$$

In (1) and (2)

$I_m(S'_m)$ = total axial current at the point S'_m on the m-th wire

$J_r(r'_m, L^u_m)$ = radial surface current density on the upper end cap of the m-th wire

$\rho(S'_m)$ = linear charge density at point S'_m on the m-th wire

$\sigma(r'_m, L^u_m)$ = radial surface charge density on the upper end cap of the m-th wire

$\hat{S}_n$ = unit vector tangential to the n-th wire at point S_n

$\hat{S}'_m$ = unit vector tangential to the m-th wire at point S'_m

$\hat{r}'_m$ = radial unit vector on the end caps of the m-th wire

L^l_m, L^u_m = lower and upper limits of the m-th wire

a_m = radius of the m-th wire

$G(S_n, S'_m)$ = approximate Green's function from a point on the axis of the m-th wire to a point on the surface of the n-th wire

$G(r'_m, L^u_m, S_n)$ = approximate Green's function from a point on the upper end cap on the m-th wire to a point on the surface of the n-th wire

The definition of the few remaining terms in (1) and (2) follows in an obvious manner.

The charge distribution on the upper end cap of the m-th wire is assumed to be uniform (the leading term in the quasi-static charge distribution) and of the form

$$\sigma(r'_m, L^u_m) = \sigma^u_m e^{j\omega t} \qquad (3)$$

where σ_m^u is the magnitude of the surface charge density. From the equation of continuity a differential equation relating the radial component of the surface current density to σ_m^u follows

$$\frac{1}{r_m}\frac{d}{dr_m}\left[r_m J_r(r_m, L_m^u)\right] = -j\omega\sigma_m^u \tag{4}$$

A solution (with a finite current at $r_m=0$) to this equation is

$$J_r(r_m, L_m^u) = -j\omega\sigma_m^u \frac{r_m}{2} \tag{5}$$

The total axial current which exists at the upper end of the m-th wire is related to the surface current density on the flat end cap by

$$I_m(L_m^u) = 2\pi a_m J_r(a_m, L_m^u) \tag{6}$$

From (5) and (6)

$$\sigma_m^u = \frac{j}{\omega}\frac{I_m(L_m^u)}{\pi a_m^2} \tag{7}$$

On the lower end cap of the m-th wire the corresponding surface charge density is

$$\sigma_m^l = -\frac{j}{\omega}\frac{I_m(L_m^l)}{\pi a_m^2} \tag{8}$$

Thus, (1) and (2) can be rewritten as

$$\phi_n(S_n) = j\frac{\eta}{4\pi k}\sum_{m=1}^{N}\left\{\int_{L_m^l}^{L_m^u} dS_m' \frac{d}{dS_m'}\left[I_m(S_m')\right] G(S_n, S_m')\right.$$

$$+ \frac{2}{a_m^2} \int_0^{a_m} dr_m' \, r_m' \left[I_m(L_m^u) G(r_m', L_m^u, S_n) - I_m(L_m^1) G(r_m', L_m^1, S_n) \right] \Bigg\} \quad (9)$$

$$A_{S_n}(S_n) = \frac{\mu}{4\pi} \sum_{m=1}^{N} \int_{L_m^1}^{L_m^u} dS_m' (\hat{S}_n \cdot \hat{S}_m') I_m(S_m') G(S_n, S_m') \quad (10)$$

In (10) the end corrections have been neglected. In many problems such terms would be most important on the n-th wire due to the $G(S_n, S_n')$ factor; i.e. it is expected that the end caps on the n-th wire will most likely affect the currents on the n-th wire more than other wires. However, in the $A_{S_n}(S_n)$ expression the $\hat{S}_n \cdot \hat{r}_m$ term will likely be zero or small unless the curvature of the wire structure is large near the ends of the wires.

Following exactly the same procedures outlined previously [3,6], the coupled set of integral equations becomes

$$\sum_{m=1}^{N} \int_{L_m^1}^{L_m^u} dS_m' I_m(S_m') \pi(S_n, S_m')$$

$$+ \sum_{m=1}^{N} \int_0^{S_n} dS_n' \left[I_m(L_m^u) G(S_n', L_m^u) - I_m(L_m^1) G(S_n', L_m^1) \right] \cos k(S_n - S_n')$$

$$+ \sum_{m=1}^{N} \frac{2}{ka_m^2} \int_0^{S_n} dS_n' \int_0^{a_m} dr_m' \, r_m' \left\{ \frac{\partial}{\partial S_n'} \left[I_m(L_m^u) G(r_m', L_m^u, S_n') - I_m(L_m^1) G(r_m', L_m^1, S_n') \right] \right\} \sin k(S_n - S_n')$$

$$- C_n' \cos kS_n - D_n' \sin kS_n = -j \frac{4\pi}{\eta} \int_0^{S_n} dS_n' E_{S_n}^{inc}(S_n') \sin k(S_n - S_n') \quad (11)$$

where

$$\pi(S_n,S_m') = (\hat{S}_n\cdot\hat{S}_m')G(S_n,S_m') - \int_0^{S_n} dS_n' \cos k(S_n-S_m')\Psi(S_n',S_m')$$

and

$$\Psi(S_n',S_m') = \frac{\partial G(S_n',S_m')}{\partial S_m'} + (\hat{S}_n'\cdot\hat{S}_m')\frac{\partial G(S_n',S_m')}{\partial S_n'} + G(S_n',S_m')\frac{\partial}{\partial S_n'}(\hat{S}_n'\cdot\hat{S}_m') \qquad (13)$$

Also,

$$C_n' = \sum_{m=1}^{N}\int_{L_m^1}^{L_m^u} dS_m'(\hat{O}_n\cdot\hat{S}_m')I_m(S_m')G(0,S_m') \qquad (14)$$

$$D_n' = \frac{4\pi D_n}{\mu} - \sum_{m=1}^{N}\frac{2}{ka_m^2}\int_0^{a_m} dr_m'\, r_m'\left[I_m(L_m^u)G(r_m',L_m^u,0) - I_m(L_m^1)G(r_m',L_m^1,0)\right] \qquad (15)$$

where $\hat{O}_n$ is the unit vector tangent to the n-th wire at $S_n=0$. Though C_n' and D_n' are treated as unknown quantities in actually solving the problem, it is necessary to have analytic expressions for them in order to check the validity of other expressions. (Notice that D_n is a constant of integration [3,6].)

In a similar manner $\phi_n(S_n)$ becomes

$$\phi_n(S_n) = -j\frac{\eta}{4\pi}C_n'\sin kS_n + j\frac{\eta}{4\pi}D_n'\cos kS_n$$

$$-j\frac{\eta}{4\pi}\sum_{m=1}^{N}\int_{L_m^1}^{L_m^u} dS_m'\, I_m(S_m')\tilde{\pi}(S_n,S_m')$$

$$+j\frac{\eta}{4\pi}\sum_{m=1}^{N}\int_{L_m^1}^{L_m^u} dS_m'\left[I_m(L_m^u)G(S_n',L_m^u)-I_m(L_m^1)G(S_n',L_m^1)\right]\sin k(S_n-S_n')$$

$$+\frac{j}{4\pi}\eta\sum_{m=1}^{N}\frac{2}{ka_m^2}\int_0^{S_n} dS_n'\int_0^{a_m} dr_m'r_m'\left\{\frac{\partial}{\partial S_n'}\left[I_m(L_m^u)G(r_m',L_m^u,S_n')-I_m(L_m^1)G(r_m',L_m^1,S_n')\right]\right\}.$$

$$\left[1-\cos k(S_n-S_n')\right]+\int_0^{S_n} dS_n'\, E_{S_n}^{inc}(S_n')\cos k(S_n-S_n') \qquad (16)$$

and

$$\tilde{\pi}(S_n,S_m') = \int_0^{S_n} dS_n'\, \Psi(S_n',S_m')\sin k(S_n-S_n') \qquad (17)$$

3. Numerical Results

To determine the unknown current distributions (11) must be solved. A useful method for solving such problems in antenna theory is the direct integration technique [7]. In particular, the numerical results have been obtained

using piece-wise constant expansion functions and point matching (or Dirac delta functions as testing functions). Also the match points are located at the end of the current zones or subsections.

The geometry of the problem used in the calculations is a set of two perpendicular crossed wires. The crossing point introduces the necessity for requiring that 1) the Kirchhoff circuit law and 2) the continuity of the scalar potential hold at the intersection of the two wires. It is convenient to define the center of the junction as the origin of the coordinate system.

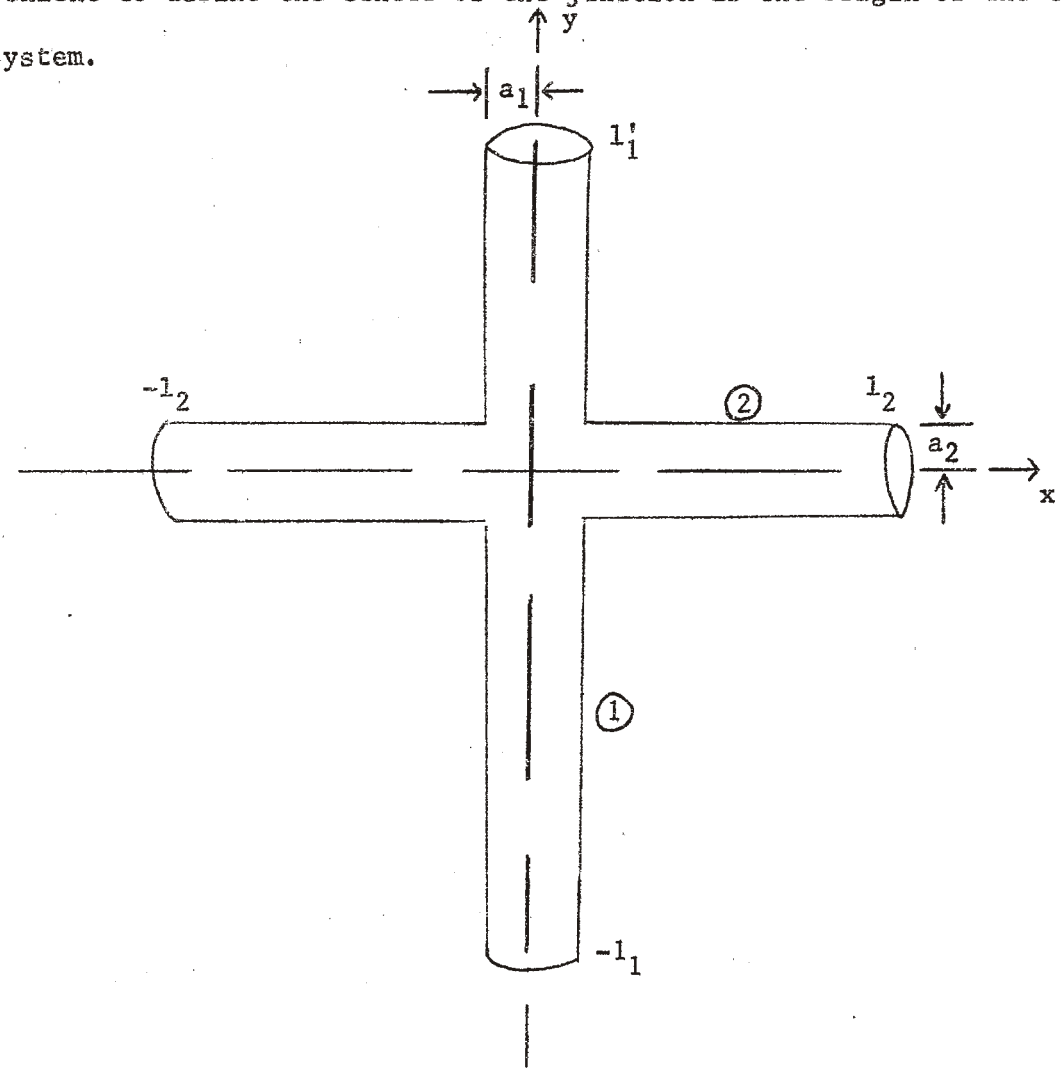

Figure 1. Perpendicular Crossed Wires

The set of coupled equations to which the above techniques were applied are

$$\int_{-l_1}^{l_1'} dy'\, I_1(y')G_{11}(y,y') - \int_{-l_2}^{l_2} dx'\, I_2(x') \int_0^y dy' \frac{\partial G_{12}(y;x')}{\partial x'} \cos k(y-y')$$

$$+ \int_0^y dy' \left[I_1(l_1')G_{11}(y;l_1') - I_1(-l_1)G_{11}(y;-l_1) + I_2(l_2)G_{12}(y,l_2) - I_2(-l_2)G_{12}(y,-l_2) \right] \cos k(y-y')$$

$$+ \frac{2}{ka_1^2} \int_0^y dy' \int_0^{a_1} dr_1'\, r_1' \left\{ \frac{\partial}{\partial y'} \left[I_1(l_1')G(r_1',l_1',y') - I_1(-l_1)G(r_1',-l_1,y') \right] \right\} \sin k(y-y')$$

$$- C_1' \cos ky - D_1' \sin ky = -j \frac{4\pi}{\eta} \int_0^y dy'\, E_y^{inc}(y') \sin k(y-y') \qquad (18)$$

and

$$\int_{-l_2}^{l_2} dx'\, I_2(x')G_{22}(x,x') - \int_{-l_1}^{l_1'} dy'\, I_1(y') \int_0^x dx' \frac{\partial G_{21}(x;y')}{\partial y'} \cos k(x-x')$$

$$+ \int_0^x dx' \left[I_1(l_1')G_{21}(x;l_1') - I_1(-l_1)G_{21}(x;-l_1) + I_2(l_2)G_{22}(x;l_2) - I_2(-l_2)G_{22}(x;-l_2) \right] \cos k(x-x')$$

$$+\frac{2}{ka_2^2}\int_0^x dx' \int_0^{a_2} dr_2' \; r_2' \left\{\frac{\partial}{\partial x'}\left[I_2(l_2)G(r_2',l_2,x')-I_2(-l_2)G(r_2',-l_2,x')\right]\right\}\text{sink}(x-x')$$

$$-C_2' \cos kx - D_1' \sin kx = -j\frac{4\pi}{\eta}\int_0^x dx' \; E_x^{inc}(x') \sin k(x-x') \qquad (19)$$

Again the assumption is made that end charge contributions on wire 1(2) will not affect directly the currents on wire 2(1). In (18) and (19) the following approximate Green's functions are used

$$G_{11}(y,y') = \frac{e^{-jk\sqrt{(y-y')^2+a_1^2}}}{\sqrt{(y-y')^2+a_1^2}}$$

$$G_{22}(x,x') = \frac{e^{-jk\sqrt{(x-x')^2+a_2^2}}}{\sqrt{(x-x')^2+a_2^2}}$$

$$G_{12}(y;x') = \frac{e^{-jk\sqrt{(y')^2+(x')^2+a_1^2}}}{\sqrt{(y')^2+(x')^2+a_1^2}}$$

$$G_{21}(x;y') = \frac{e^{-jk\sqrt{(x')^2+(y')^2+a_2^2}}}{\sqrt{(x')^2+(y')^2+a_2^2}}$$

$$G(r_1',l_1',y') = \frac{e^{-jk\sqrt{(y'-l_1')^2+(r_1')^2}}}{\sqrt{(y'-l_1')^2+(r_1')^2}}$$

$$G(r_2',l_2,x') = \frac{e^{-jk\sqrt{(x'-l_2)^2+(r_2')^2}}}{\sqrt{(x'-l_2)^2+(r_2')^2}}$$

Due to the existence of an electromagnetic symmetry plane [8], the analysis is performed in terms of E- and H-polarization modes, symmetric and anti-symmetric [3]. Also this allows one to make direct comparison to previously obtained results from thin wire theory [3].

4. Graphical Presentation

As has been pointed out, results have been obtained for a configuration of open-ended, perfectly conducting thin straight tubes which intersect perpendicularly [3]. These results indicate that large instabilities appear in the current and charges distributions as the tubes (wires) become thicker. In order to illustrate the effectiveness of including the additional end correction terms, the results presented here are obtained for the same basic geometry as the results presented in [3]. Accordingly, the basic structure parameters in this analysis are defined as:

$$l_1'/l_1 = 0.5 \qquad 2l_2/(l_1'+l_1) = 1.0 \qquad kl_2 = 1.15$$

Excitation of the thick wire structure is accomplished in exactly the same manner as it was in the thin wire analysis. All of the results presented are for normal incidence only.

Figures 2-4 give the magnitudes of the current distributions on each of the elements of the thick wire structure as a function of position for E-polarization, symmetric mode; i.e. the incident E field is directed along wire 1

(see reference [3]). Figure 5 gives the magnitude of the current distribution on wire 2 for H-polarization, antisymmetric mode; i.e. the incident E field is directed along wire 2 (see reference [3]). Figure 6 exhibits the dependence of the linear charge distribution on position. This particular curve gives the linear charge distribution on wire 2 for E-polarization, symmetric mode. The charge distributions on the other elements are not presented, but they do exhibit essentially the same functional behavior.

The currents and charges are normalized with respect to the magnitude of the incident electric fields, E_o, and the total length of wire 2, $2l_2$. The linear charge distributions were calculated from the current distributions according to the equation of continuity.

From the data that are presented it is readily observed that including end effects yields a much smoother current distribution on the wires plus there is a slight shift in the current amplitude. The latter effect is expected since the addition of end plates increases the effective length of the wire by an amount exactly equal to the wire radius. The calculation of the charge density with end plates on the wires yields a much smoother distribution; however there is yet some oscillation present. This oscillation is probably spurious and probably appears because the assumed uniform charge distribution is not accurate enough.

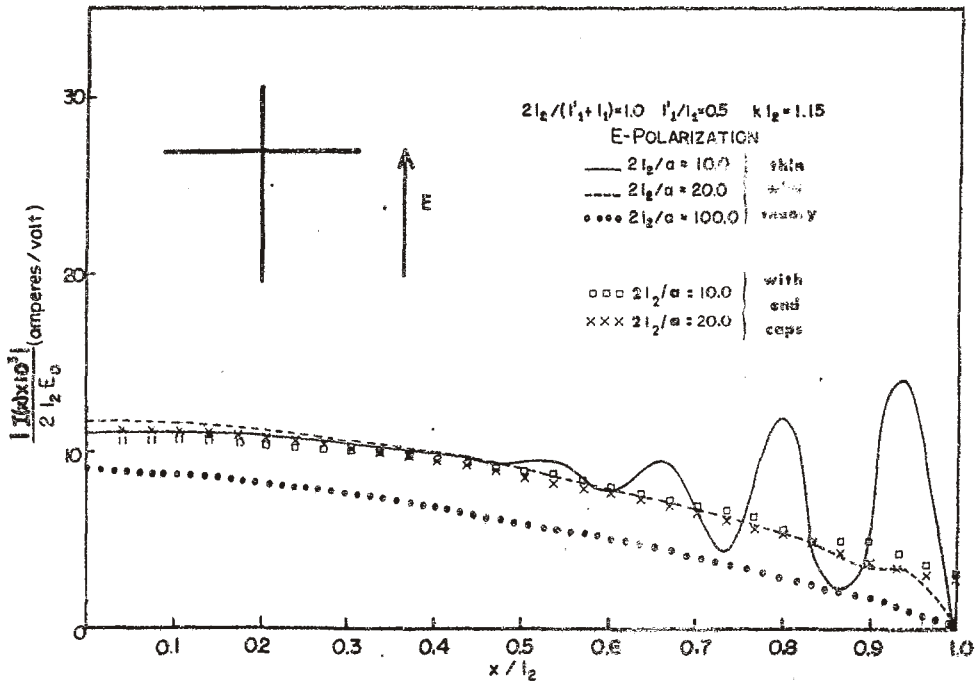

Figure 2. Currents on wire 2 vs x/l_2.

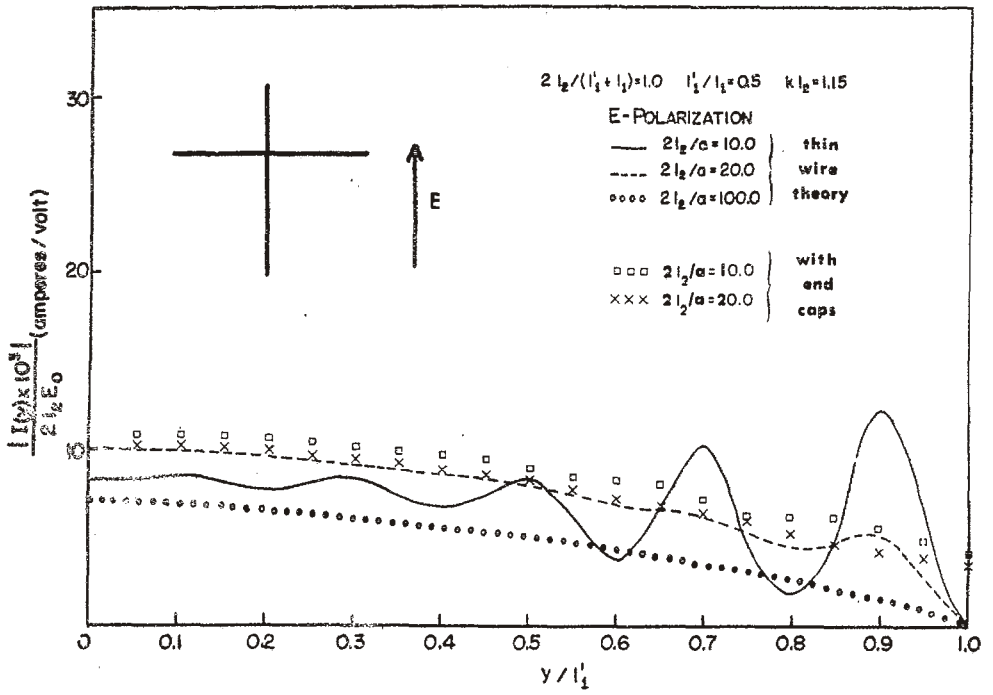

Figure 3. Currents on wire 1 ($y > 0$) vs y/l_1'.

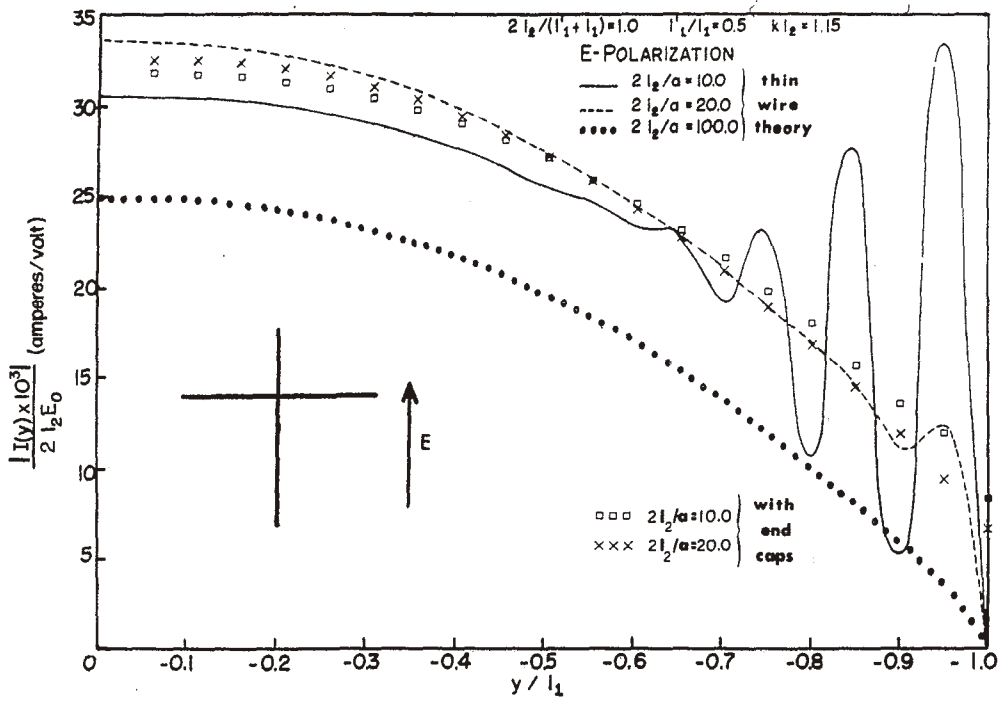

Figure 4. Currents on wire 1 ($y < 0$) vs y/l_1.

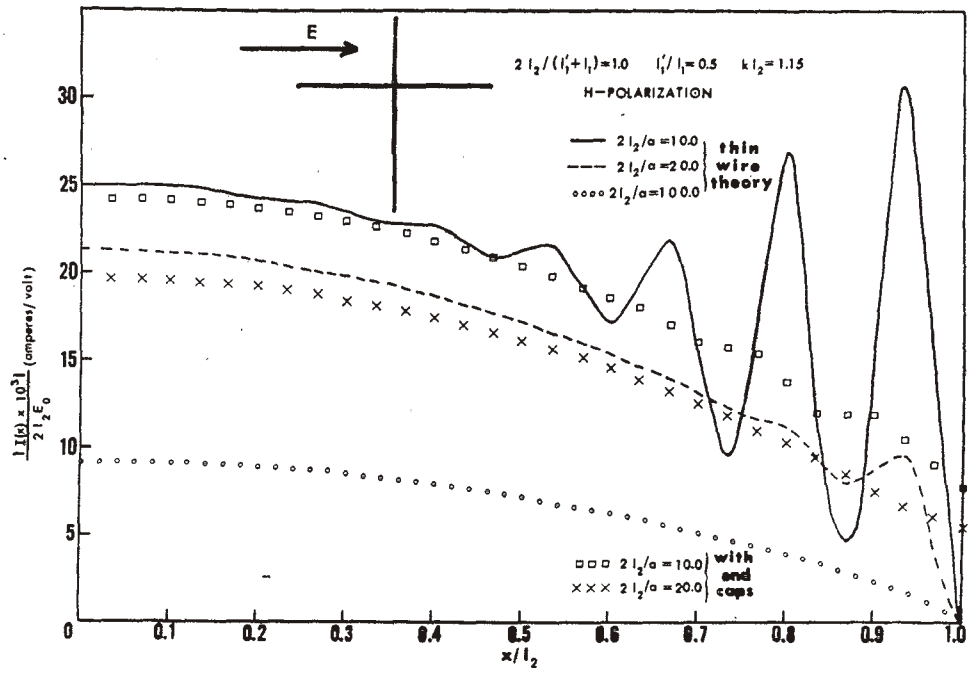

Figure 5. Currents on wire 2 vs x/l_2.

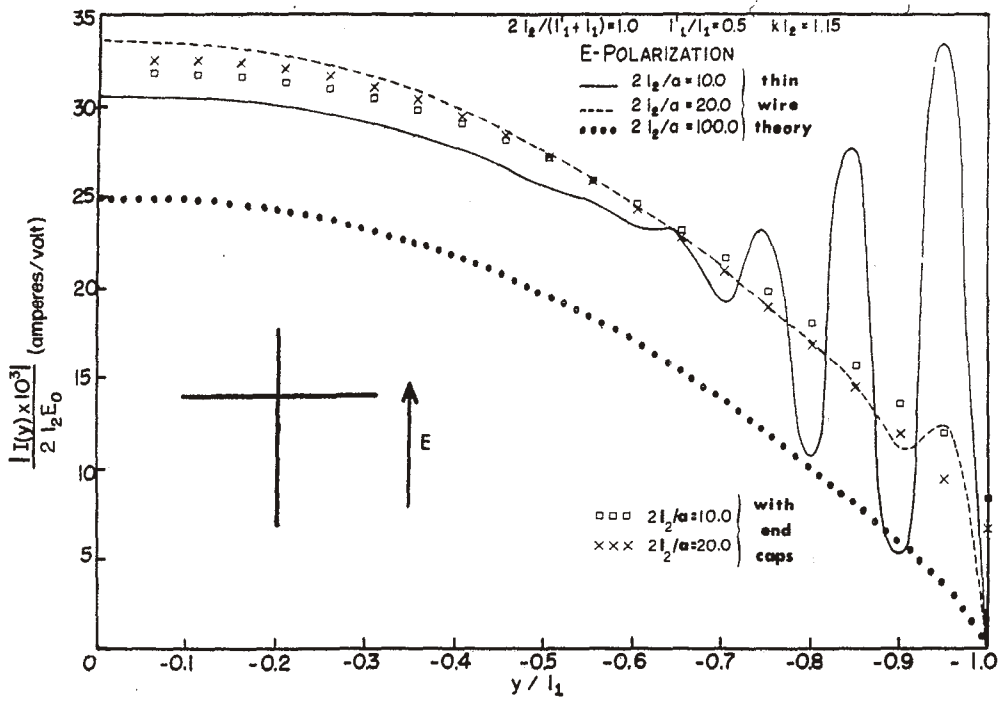

Figure 4. Currents on wire 1 ($y < 0$) vs y/l_1.

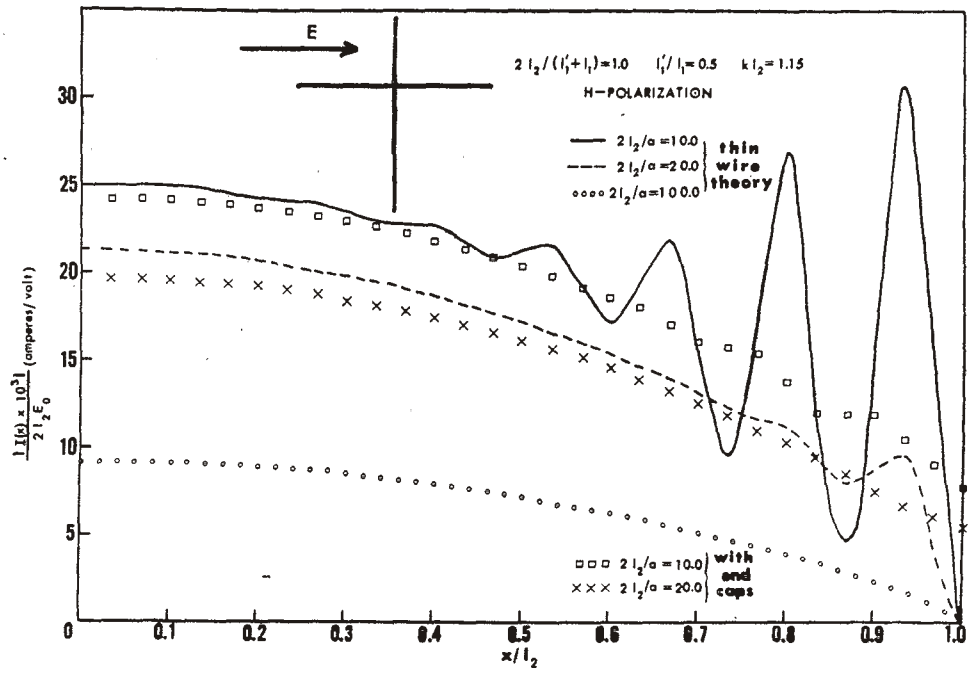

Figure 5. Currents on wire 2 vs x/l_2.

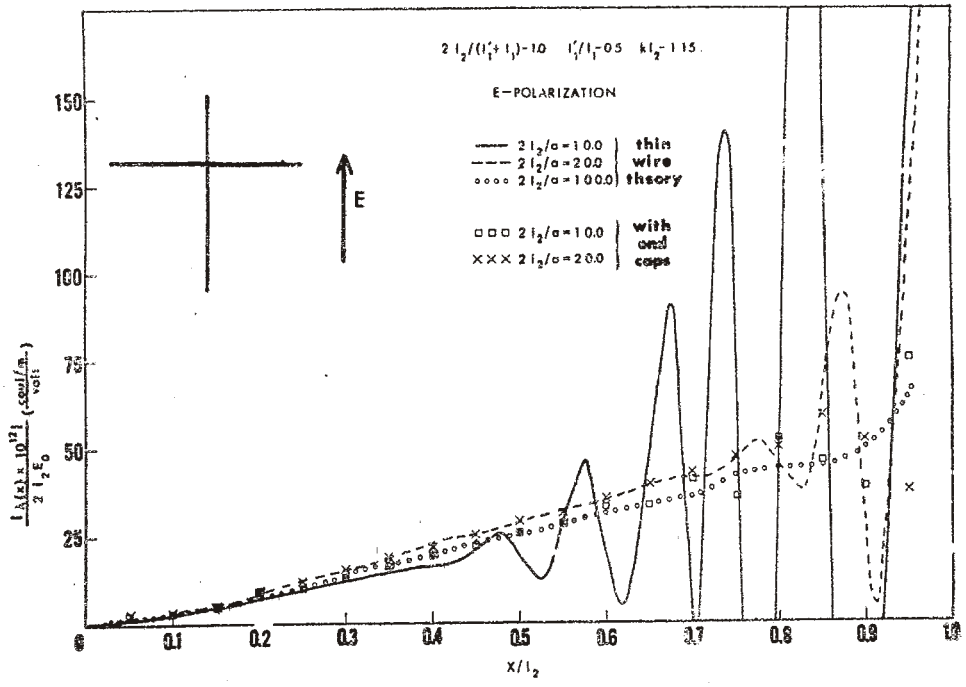

Figure 6. Linear charge density on wire 1 (y 0) vs y/l_1.